Identifying the Azobenzene/Aniline Reaction Intermediate on TiO_2-(110): a DFT Study

M.K. Bradley, J. Robinson, D.P. Woodruff*

Physics Department, University of Warwick, Coventry CV4 7AL, UK

Abstract

Density functional theory (DFT) calculations, both with and without dispersion corrections, have been performed in order to investigate the nature of the common surface reaction intermediate that has been shown to exist on TiO_2(110) as a result of exposure to either azobenzene ($C_6H_5N{=}NC_6H_5$) or aniline ($C_6H_5NH_2$). Our results confirm the results of an earlier DFT study that dissociation of azobenzene into two adsorbed phenyl imide (C_6H_5N) fragments, as was originally proposed, is not energetically favourable. We also find that deprotonation of aniline to produce this surface species is even more strongly energetically disfavoured. A range of alternative surface species have been considered, and while dissociation of azobenzene to form surface C_6H_4NH species is energetically favoured, the same surface species cannot form from adsorbed aniline. On the contrary, adsorbed aniline is much the most stable surface species. Comparison with experimental determinations of the local adsorption site, the Ti-N bondlength, the molecular orientation and the associated C 1s and N 1s photoelectron core level shifts are all consistent with the DFT results for adsorbed aniline, and are inconsistent with other adsorbed species considered. Possible mechanisms for the hydrogenation of azobenzene required to produce this surface species are discussed.

Keywords: surface reaction; heterogeneous catalysis; hydrogenation; dehydrogenation

*Corresponding author: tel +44 2476 523378 ; email d.p.woodruff@warwick.ac.uk

1. Introduction

In recent years there has been growing interest in the properties of Au nanoparticles on TiO_2 following the discovery that this system is an effective catalyst for low-temperature oxidation of CO.[1] More recently TiO_2/Au has also been found to act as a high-yield catalyst in the synthesis of aromatic compounds [2,3] including the synthesis of azobenzene ($C_6H_5N=NC_6H_5$) via oxidation of aniline ($C_6H_5NH_2$) (see Fig. 1).

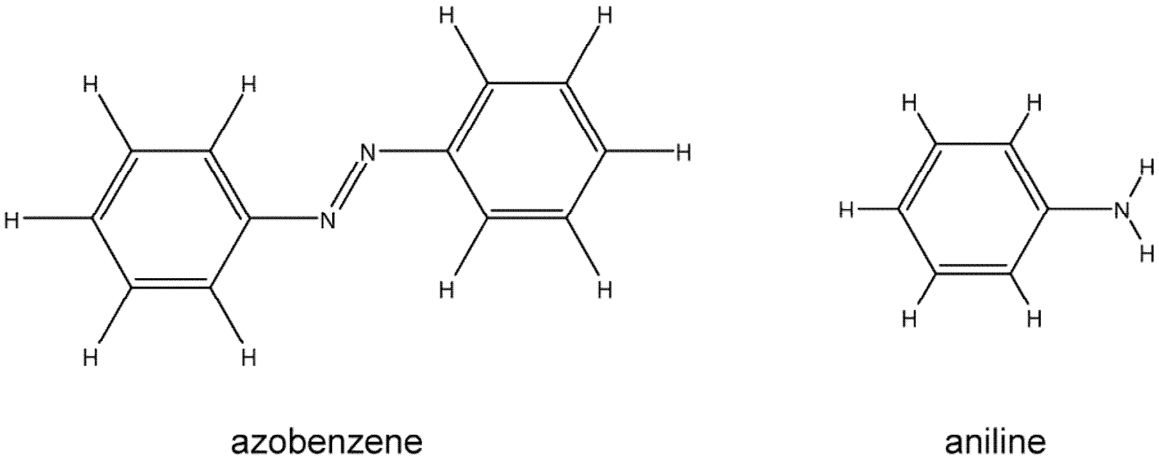

Fig. 1 The (*trans*) azobenzene and aniline molecules.

However, it has also been found [3] that TiO_2 *in the absence of the Au nanoparticles* was also effective, and highly selective, in azobenzene synthesis. This led to a careful UHV surface science study of the interaction of azobenzene and aniline with both the rutile-phase TiO_2(110) and anatase-phase TiO_2(101) surfaces by Li, Diebold and coworkers [4,5] who found evidence for a single surface reaction intermediate, produced by interaction with either azobenzene or aniline, on both surfaces. On the rutile TiO_2(110) surface they found that adsorption of either molecule at full coverage leads to the formation of a c(2x2) 0.5 ML ordered molecular phase, as seen both with low energy electron diffraction (LEED) and scanning tunnelling microscopy (STM). The STM images appear to be independent of the initial reactant molecule, as do the X-ray photoelectron spectroscopy (XPS) data from both the substrate atoms and the molecular constituent atoms.[4] Ultraviolet photoelectron spectroscopy (UPS) data have also been interpreted in terms of a common surface intermediate with both reactants on both forms of titania.[5]

The common molecular adsorbate species was assigned to phenyl imide (C_6H_5N-), produced either by N=N bond scission of azobenzene, or by dehydrogenation of aniline.

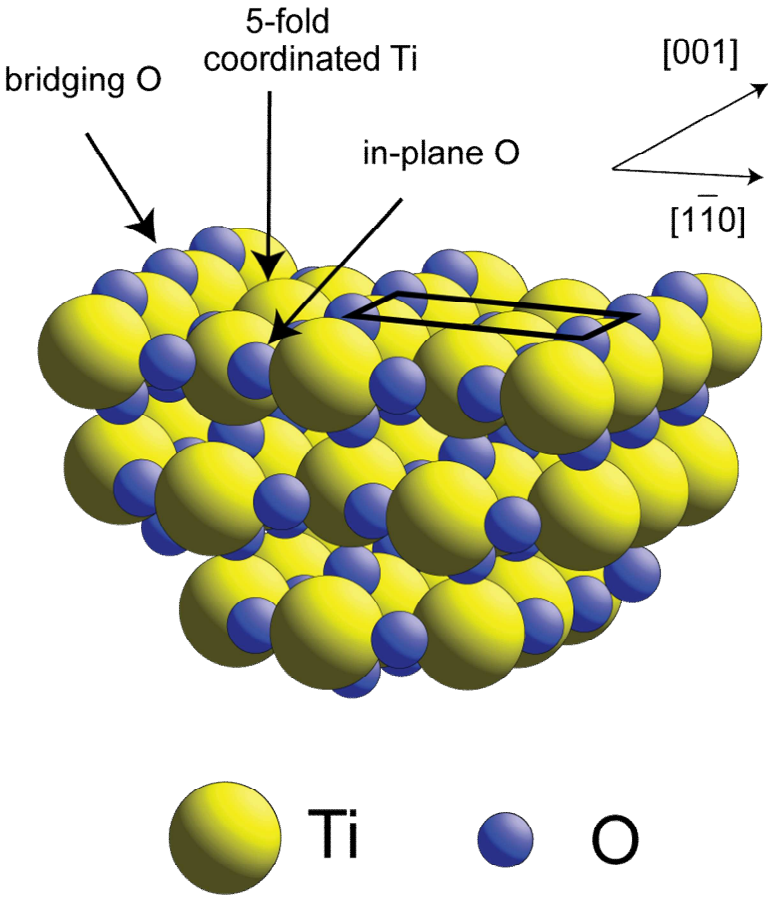

Fig. 2 Schematic diagram of the TiO_2(110) surface showing the different surface atoms, the azimuthal directions within the surface and the (1x1) unit mesh.

A subsequent experimental investigation of the interaction of azobenzene and aniline with the rutile TiO_2(110) surface by scanned-energy electron diffraction (PhD) [6,7] and by near-edge X-ray absorption fine structure (NEXAFS) has provided further confirmation of the existence of a common molecular surface intermediate.[8] C K-edge NEXAFS data show this species retains a phenyl ring (the molecular plane of which is tilted relative to the surface normal and not aligned along either principal azimuth) while it bonds to the surface though a N atom that lies atop the undercoordinated (5-fold coordinated) surface Ti atoms (Fig. 2). There is, however, an ambiguity in the PhD data interpretation

regarding the Ti-N bondlength; two values, 1.77±0.05 Å and 2.27±0.04 Å are found to be equally consistent with the experimental data, but the former value was proposed to be more consistent with the expected Ti=N double bond in this geometry.

The dissociation of azobenzene to phenyl imide on TiO_2(110) has recently been investigated using density functional theory (DFT).[9,10] In qualitative agreement with the PhD structural study, the phenyl imide species is found to bond to the surface through the N atoms in a local Ti-atop site. However, the Ti-N bondlength found in the DFT study of 2.07 Å is not consistent with the PhD investigation, nor is the fact that in the DFT study the phenyl ring is found to lie perpendicular to the surface and parallel to the $[0\bar{1}1]$ azimuth. Even more significantly, the DFT calculations indicate that the energetics should not favour dissociation of the azobenzene into two phenyl imide species on the surface; in fact an energy increase of 2.73 eV is found to be necessary to effect the dissociation. Including the role of van der Waals interactions in DFT-D calculations significantly increases the adsorption energies of both azobenzene and phenyl imide, but actually leads to an even larger energy of 3.12 eV [9] (or 3.29 eV [10]) to overcome in order to create the adsorbed phenyl imide species. Notice that the inclusion of the dispersion correction in these calculations also leads to a change in the preferred geometry of adsorbed intact azobenzene; both DFT and DFT-D calculations show the *trans* configuration to be energetically favoured in the free molecule, but while DFT favours the *cis* form in the adsorbed species, DFT-D favours adsorbed *trans*-azobenzene. Our own results reproduce this conclusion. A numerical error in one of the tables of the original publication [10] actually led to a different conclusion being reported.[11]

Here we present the results of a new DFT study. Our original motivation of the work (started prior to the recent DFT publications) was to determine the optimum geometry of the phenyl imide species to compare with the results of the PhD study, but having also found that the energetics should not favour the dissociation of either azobenzene or aniline, we have explored alternative interpretations of the surface reaction and the associated molecular intermediate. Our results lead to the surprising conclusion that much the most energetically-favoured surface species is adsorbed aniline, the local geometry of

which is fully consistent with the results of the recent PhD and NEXAFS studies. We also explore other information from UPS and XPS that may cast further light on this issue.

2. Computational details

Our DFT calculations were performed using the plane wave pseudopotential code CASTEP [12] in the generalised gradient approximation (GGA). The Perdew and Wang exchange and correlation functional (PW91) [13] was used for most of the calculations, but some additional calculations including the role of van der Waals interactions were performed using the DFT-D implementation in CASTEP, using the PW91 functional with the OBS (Ortmann, Bechstedt and Schmidt [14]) scheme,[15] in order to check the role of dispersion forces which have been shown to have a very significant effect on the absolute adsorption energies.[9,10] Total energy calculations were conducted using ultrasoft pseudopotentials from the CASTEP pseudopotential library to minimise computation time. In addition, C and N ultrasoft pseudopotentials were constructed using the CASTEP on-the-fly pseudopotential generator, both with and without a 1s electron removed, in order to determine accurately the relative 1s photoelectron electron binding energies using the method described by Gao *et al.*[16] These C and N pseudopotentials were constructed using core radii of 1.4 Å and 1.5 Å respectively, in each case using two non-local ultrasoft projectors for the 2s and 2p channels.

Calculations for the adsorbed molecular fragment, and for adsorbed intact aniline, were based on the $\begin{bmatrix} 2 & 0 \\ 1 & 1 \end{bmatrix}$ primitive unit mesh of the c(2x2) structure using single-sided slabs comprising 4 TiO_2 trilayers (each tri-layer containing one Ti layer and two O layers), with the lower 2 trilayers fixed to the geometry determined in a bulk calculation. This slab thickness (with a vacuum gap in excess of 9.5 Å for all adsorption structures) was found to give good convergence, consistent with the results of an earlier study of adsorbed hydrogen.[17] A kinetic energy cut-off of 420 eV and 2x2x1 Monkhorst-Pack k-point sampling mesh were used. The bulk calculations yielded structural parameters of a = 4.640 Å, c = 2.965 Å, u = 0.305, the lattice parameters being within 1% of the

experimental values a = 4.594 Å, c = 2.959 Å, u = 0.305 [18]. A larger $\begin{bmatrix} 4 & 0 \\ 2 & 2 \end{bmatrix}$ primitive unit mesh of a c(4x4) structure was used for calculations of the (larger) adsorbed intact azobenzene molecule, and also in a subset of additional calculations to provide some indication of the importance of intermolecular interactions.

In order to obtain absolute adsorption or formation energies total energy calculations of isolated azobenzene and aniline molecules, and of the phenyl imide radical, were performed in unit cells of dimensions 14x14x10 $Å^3$ for the imide and aniline, and 18x16x10 $Å^3$ for azobenzene. The PW91 calculations found the free aniline molecule to be 1.531 eV more stable than half the energy of an isolated azobenzene molecule plus a H_2 molecule, and 3.525 eV more stable than a free phenyl imide radical plus a H_2 molecule. The energy cost to dissociate gas-phase azobenzene into two phenyl imide free radicals is thus (3.525-1.531)x2 = 3.988 eV (or 1.994 eV per phenyl imide radical), while the energy cost to deprotonate aniline to phenyl imide in the gas phase is 3.525 eV. When adsorbed on the titania surface, of course, these values may be very different.

3. Results

3.1 Energetics and structure

Calculations were first performed to identify the most favourable geometry for phenyl imide, C_6H_5N-, in a c(2x2) structure on TiO_2(110). An extensive range of plausible adsorption geometries were explored, leading to eight distinct optimised structural models involving different local sites and molecular orientations, each corresponding to a local energy minimum in the potential energy surface. Consistent with the results of Prates Ramalho and Illas,[9] we find the lowest-energy structure to correspond to adsorption through the N atom atop the five-fold-coordinated surface Ti atoms, with molecular plane perpendicular to the surface and parallel to the $[0\bar{1}1]$ azimuth (Fig. 3). In contrast to the earlier finding of Ti-N bondlength of 2.07 Å, our calculations find this bondlength to be 2.22 Å, a value which is reduced to 2.17 Å with the inclusion of van der Waals interactions in the DFT-D calculations. One curious feature of this adsorption

structure is that there are two unpaired spins on the N atom, so the molecule has a magnetic moment of $2\mu_B$; our calculations reveal that this is also a property of the free phenyl imide radical. A check on the relative energies in the adsorption structure of different ordering of the spins in a larger unit mesh indicates that the layer is paramagnetic rather than ferro- (or antiferro-) magnetic. We have established through communication with the authors that this same effect was also found to be a feature of the minimum energy structure found by Prates Ramalho and Illas.[9]

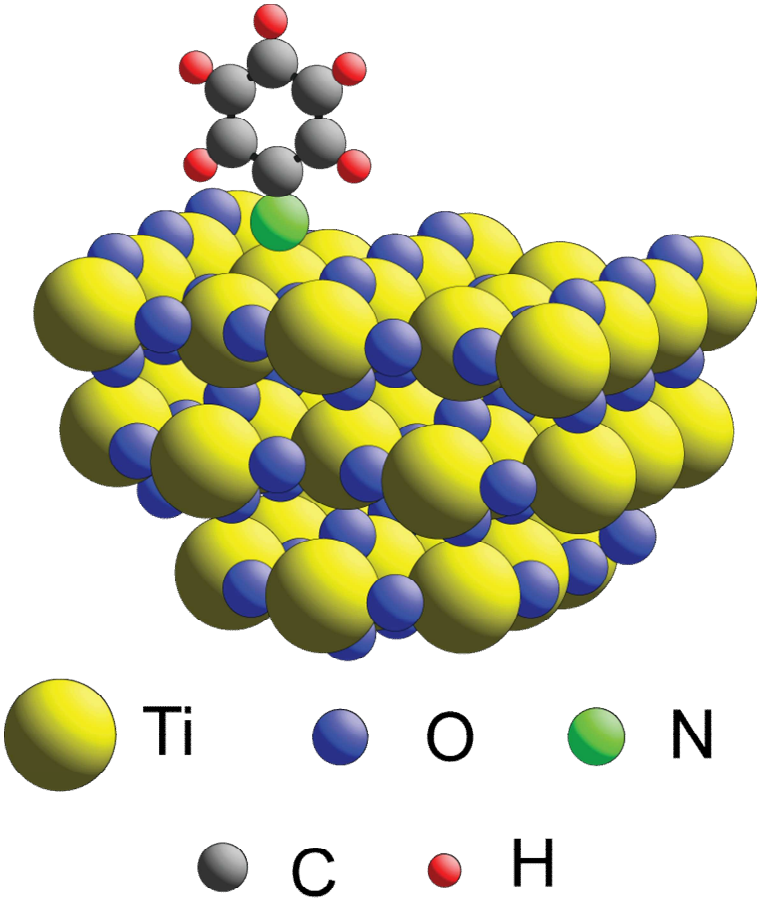

Fig. 3 Schematic diagram of the phenyl imide adsorption geometry. For clarity only one adsorbed species is shown.

In the standard DFT calculations we find the phenyl imide to be adsorbed in a c(2x2) overlayer with a total energy lower than that of the free gas-phase radical by 0.773 eV, implying that this adsorbed species is still 1.221 eV per adsorbed species less favourable

than one half of a gas-phase azobenzene molecule. In the DFT-D calculations that included the correction for dispersion forces the adsorption energy of the free radical was increased to 1.319 eV, but this was still 0.737 eV less favourable than half the energy of the gas-phase azobenzene molecule. Note that adsorption structures involving phenyl imide in a bridging site, bonding to two adjacent undercoordinated surface Ti atoms (as originally speculated [4]), had adsorption energies of 0.640-0.760 eV less than that of the favoured atop site and so are found to be extremely weakly bonded to the surface (by <~100 meV) relative to the gas-phase free radical. The main conclusion is therefore that while the preferred adsorption site is consistent with the PhD experiments (and the bondlength discrepancy may also be acceptable), the energetics clearly indicate that azobenzene should not dissociate in this way in TiO_2(110). We may also note that this energetic problem is even more serious for the interaction of the surface with aniline to produce the same surface species, as demonstrated below.

We have therefore explored alternative possible adsorbed species and their associated adsorption geometries and energies. For each adsorbate species considered the only constraint applied was that the N atom of the adsorbate was approximately atop a 5-fold coordinated Ti atom of the substrate as required to be consistent with the experimental PhD result; however, the Ti-N bondlength and molecular orientation were unconstrained. We focussed first on alternative species having the same stoichiometry as phenyl imide that might arise from breaking the N=N bond of azobenzene. Specifically, in addition to the phenyl imide species, C_6H_5N-, we considered the possibility that one of the phenyl H atoms is transferred to the N to produce C_6H_4NH, that one of these H atoms is removed to produce a C_6H_4N species, leading either to coadsorption with the H atom, or to loss of this H atom into the gas phase as H_2, or finally that two of the phenyl H atoms are transferred to the N atoms to produce a $C_6H_3NH_2$ species. Table 1 summarises the main parameters associated with the lowest-energy adsorption geometries of these different species. In all cases the adsorption energy is expressed relative to (one half of) the energy of the intact gas-phase azobenzene molecule.

Model	E rel. to ½ azobenzene + clean surface (eV)	Total spin magnetic moment (μ_B)	N-Ti bond length (Å)
C_6H_5N	1.221 (*0.737*)	2.00	2.22 (*2.17*)
C_6H_4NH	-0.663 (*-1.356*)	0	1.94 (*1.94*)
C_6H_4N +1/2$(H_2)_g$	0.879	0.98	1.85
C_6H_4N +H_a	0.317	0	1.76
$C_6H_3NH_2$	1.922	0.95	2.45
$C_6H_5N{=}NC_6H_5$	-0.308(*-0.795*)	0	2.48(*2.70*)

Table 1 Adsorption energies, spin moments and N-Ti bondlengths for adsorption on TiO_2(110) of different species having the same stoichiometry as one half of an azobenzene molecule. The main values are based on standard DFT GGA calculations without dispersion corrections, but the bracketed values in italics are from DFT-D calculations. For consistency with the other values in the table the adsorption energy for intact azobenzene has been divided by a factor of 2 and is the energy difference between the most stable isomer in the gas phase (*trans*) and the most stable isomer (*cis* in DFT and more *trans*-like in DFT-D) in the adsorbed phase; note that the N-Ti bondlength difference in the DFT (PW91) and DFT-D calculation is at least in part due to the different adsorption geometries found, with two N atoms bridging two surface Ti atoms, or with only one N atom (much closer to the surface than the second N atom) bonding to a surface Ti atom, respectively.

As may be seen from the table, three of these species have a lower energy than the phenyl imide species considered originally, and one of them, C_6H_4NH, has an energy that is actually consistent with the dissociation of the azobenzene molecule being favoured on the surface by 0.633 eV relative to half the energy of intact azobenzene (this value increasing to 1.356 eV after inclusion of dispersion forces). This species, like all of the lowest-energy structures of Table 1, has the N atom bonded to a single undercoordinated surface Ti atom; the local geometry is shown in Fig. 4. As is clear from the figure, the bonding to the substrate involves not only the N atom located near-atop a surface Ti, but

also the deprotonated C atom of the phenyl ring which bonds to a bridging O atom of the surface with a C-O bondlength of 1.38 Å. Like the phenyl imide adsorption geometry (Fig. 3) the molecular plane is perpendicular to the surface and aligned in the $[0\bar{1}1]$ azimuth.

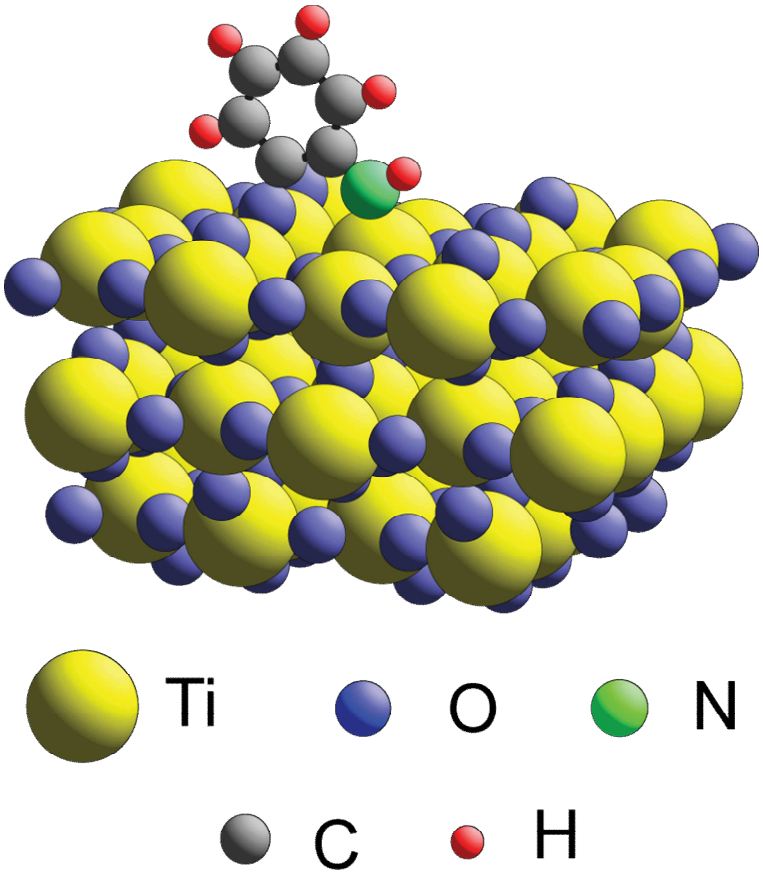

Fig. 4. Schematic diagram of the C_6H_4NH adsorption geometry. For clarity only one adsorbed species is shown, but the diagram is taken from a calculation of a c(2x2) overlayer and the substrate rumpling shows this periodicity.

This molecular orientation is not consistent with the results of the NEXAFS experiments. Moreover, while the fact that the N lies close to atop a surface Ti atom is consistent with the PhD experiments, the Ti-N bondlength of 1.94 Å lies roughly midway between the two possible values derived from the PhD study. There is one further problem with this energetically preferred structure that is based on the stoichiometry of half an azobenzene

molecule. Specifically, while the energetics favour the dissociation of azobenzene into two such adsorbed C_6H_4NH species, the energy of this surface species plus an H_2 molecule is still greater by 0.871 eV (0.312 eV in DFT-D) than that of a free aniline molecule, so this species should not be formed by the reaction of aniline with the TiO_2(110) surface.

Model	E rel. to aniline + clean surface (eV)	Total spin magnetic moment (μ_B)	N-Ti bond length (Å)
$C_6H_5N + (H_2)_g$	2.752 (*2.406*)	2.00	2.22 (*2.17*)
$C_6H_5N + H_a + ½ (H_2)_g$	1.435	1.00	1.90
$C_6H_5N + 2H_a$	0.630	0	1.75
$C_6H_4NH + (H_2)_g$	0.871 (*0.312*)	0	1.94 (*1.94*)
$C_6H_4NH + H_a + ½(H_2)_g$	0.858	0	1.96
$C_6H_5NH + ½(H_2)_g$	0.763	1.00	2.23
$C_6H_5NH + H_a$	-0.022 (*-0.720*)	0	1.92 (*1.92*)
$C_6H_5NH_2$	-0.896 (*-2.165*)	0	2.38 (*2.29*)

Table 2 Adsorption energies, spin moments and N-Ti bondlengths for adsorption on TiO_2(110) of different species having the same stoichiometry as an aniline molecule. The main values are based on standard DFT GGA calculations without dispersion corrections, but the bracketed values in italics are from DFT-D calculations.

In order to address this problem we have therefore explored possible surface species associated with the reaction of aniline with TiO_2(110) for which the initial stoichiometry differs from that of half an azobenzene molecule by the addition of two further H atoms. In particular, not only do we need to consider the possibility of a phenyl imide species coadsorbed with one or both of the H atoms removed from the N, or of only partial dehydrogenation of the NH_2 group of aniline to produce an adsorbed C_6H_5NH plus hydrogen on the surface or in the gas phase, but also of adsorbed intact aniline. The results of the associated optimised geometries are summarised in Table 2.

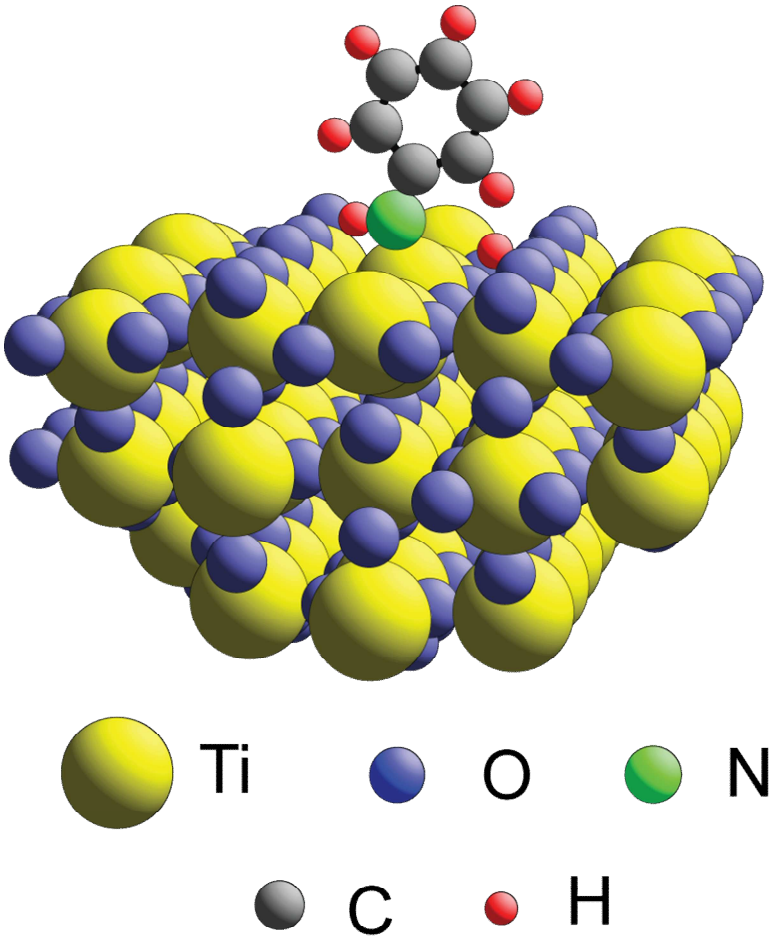

Fig. 5. Schematic diagram of the $C_6H_5NH+H_a$ adsorption structure. For clarity only one adsorbed molecular species and the associated atomic H atom is shown.

Notice that for those species found to have unpaired spins when adsorbed in isolation, the total energy is lowered very significantly (as is the spin moment) if hydrogen atoms that are removed from the aniline are adsorbed onto the surface instead of being desorbed into the gas phase. The energy gains associated with these adsorbed H atoms are very much larger than the adsorption energy of H on the surface relative to gas-phase H_2 which is only ~0.1-0.2 eV/H atom.[17,19] Only one partially-dissociated adsorbed species is found to be energetically preferred over the intact gas-phase aniline molecule, namely C_6H_5NH coadsorbed with atomic H. This structure is shown in Fig. 5; as for the previously-considered species, bonding is through the N atom in a near-atop site above a surface Ti

atom, and the molecular plane lies perpendicular to the surface and parallel to the [0$\bar{1}$1] azimuth. The H atom bonds to a bridging O atom to produce a local hydroxyl species, as in hydrogen adsorption on the bare surface. Notice that in the standard DFT calculations the energetic preference for this structure over the gas-phase aniline is very marginal (only 22 meV). However, DFT-D calculations, including dispersion corrections, increase this energetic preference to a far more significant value of 0.72 eV. The trend of dispersion corrections substantially increasing adsorption energies in this system is consistent with the results of Prates Ramalho and Illas for azobenzene and phenyl imide.[9,10] Our calculations indicate, however, that while the absolute energies are influenced quite significantly by the dispersion corrections, the relative ordering of the energies of the different structures explored is not. The only exception to this statement concerns the *trans* and *cis* configurations of adsorbed intact azobenzene.

What is also clear from Table 2, however, is that much the most energetically favourable adsorption structure to form following exposure of the surface to aniline is that of the intact aniline molecule. In the standard DFT calculation the adsorption of intact aniline is favoured over the gas phase by almost 0.9 eV per molecule, and this value increases after inclusion of dispersion forces to more than 2.1 eV. The associated adsorption geometry is shown in Fig. 6. The molecule is bonded to the surface through the N atom that occupies an off-atop site above a surface Ti atom, but the molecule is tilted by 45° relative to the surface (35° in DFT-D) and twisted by ~25° relative to the [001] azimuth. This molecular orientation is in excellent agreement with the experimental NEXAFS data, while the adsorption site is consistent with the PhD results. The Ti-N bondlength of 2.29 Å (in DFT-D) is also in complete agreement with the longer of the two possible values found in the PhD experiments of 2.27±0.04 Å. Intermolecular interactions seem likely to play a role in the tilt and twist of the adsorbed aniline, although van der Waals interactions between the phenyl ring and the underlying surface also appear to cause the molecule to lie flatter on the surface.

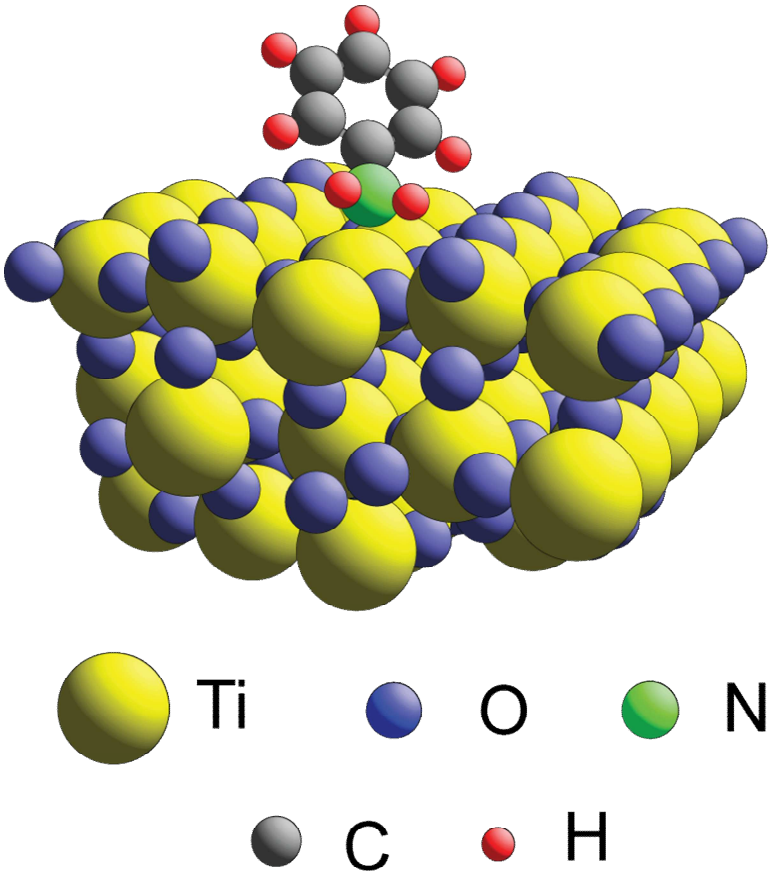

Fig. 6. Schematic diagram of the aniline adsorption structure. For clarity only one adsorbed molecular is shown.

A clear conclusion is thus that the interaction of aniline with TiO_2(110) may be expected to lead to the adsorption of intact aniline, and that the local geometry of this species is consistent with the existing experimental structural information regarding the N adsorption site, the Ti-N bondlength, and the molecular orientation. By contrast, our calculations would suggest that the favoured adsorption state arising from the interaction of pure azobenzene with TiO_2(110) is C_6H_4NH. However, the molecular orientation of this species on the surface is not consistent with the experimental NEXAFS data, nor is the Ti-N bondlength in agreement with the experimental PhD data. Furthermore, all experimental data available so far indicates that interaction with these two molecules leads to the formation of the same adsorbed species in the same local geometry. One

possible solution to this dilemma is that molecular aniline is the adsorbed species in both experiments. Note that this state is energetically preferred over C_6H_4NH for interaction with azobenzene *in the presence of a source of hydrogen*. Specifically adsorbed aniline is energetically more favourable than half the energy of gas-phase azobenzene plus one gas-phase H_2 molecule (by 2.472 eV in the standard (PW91) DFT calculation, and by 3.842 eV in the DFT-D calculation). Of course, a key question is whether such a source of hydrogen could be present in the reported experiments on this system. Before considering this question further, however, we explore the possible use of our DFT calculations to compare information available on the electronic structure of the surface from theory and experiment.

3.2 Electronic structure information

While the experimental structural data provides the most obvious basis for comparison with the results of the DFT calculations, the electronic structure associated with the different adsorbed species can lead to distinct spectroscopic signatures, and experimental UPS [5] and XPS [4,8] data have been reported.

Fig. 7 shows a comparison of experimental UPS data with the calculated local density of state (LDOS) obtained from the DFT calculations. To allow a more direct comparison of theory and experiment the calculated LDOS have been convoluted with a Gaussian function with a sigma value of 0.4 eV which leads to peaks with a similar width to those of the experimental spectra. In order to give some indication of the reliability of the relative energies in these calculations, a comparison of the LDOS for a free aniline molecule with the gas-phase photoemission spectrum [20] is shown on the left. Below the gas-phase spectrum are three sets of vertical lines; the bottom two correspond to the energy levels calculated from ab initio molecular orbital (MO) theory in the original gas-phase publication [20] using two different schemes (minimal basis set (SZ) and double zeta (DZ)), while the upper set of lines are estimates of the actual energies of these states in the UP spectrum. This latter set of lines is repeated above the experimental UP spectrum. Above the gas-phase photoemission spectrum are shown the results of the present

calculations as a broadened LDOS and, immediately below, a set of vertical lines corresponding to the peak positions in the unbroadened calculated LDOS.

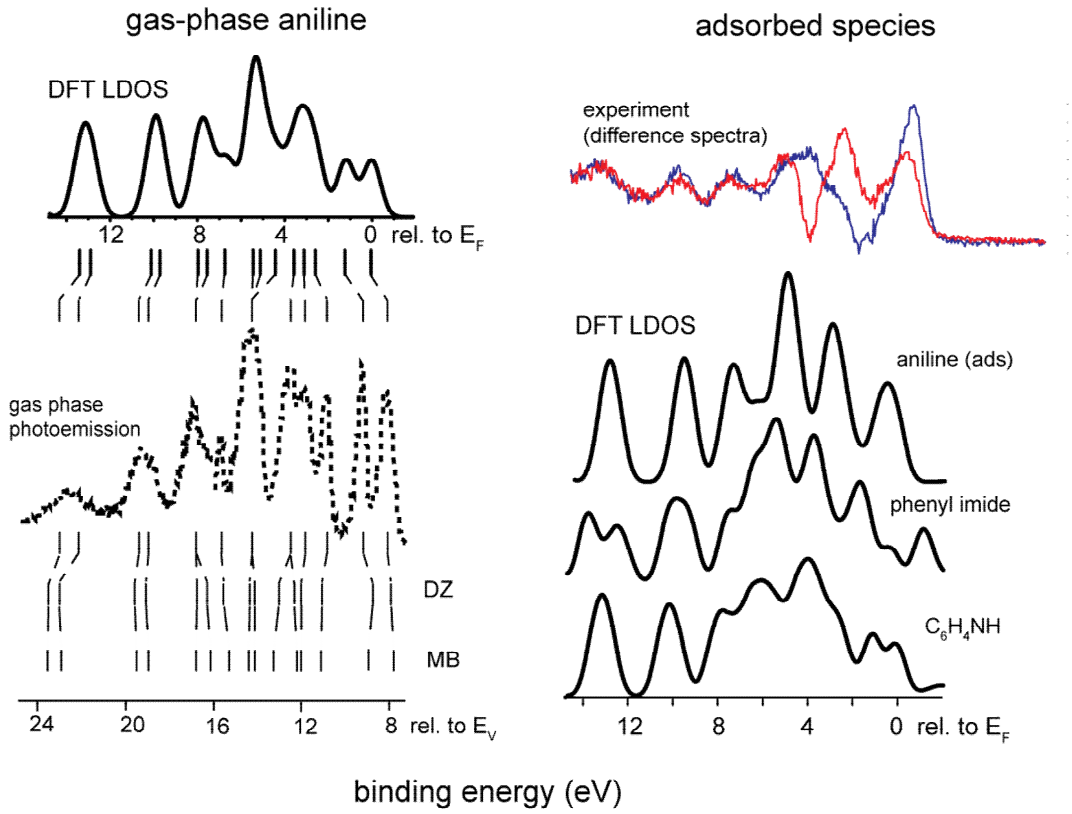

Fig. 7. Comparison of UP spectra from gas-phase aniline, and UP difference spectra from the surface species produced on TiO_2(110) by exposure to azobenzene, with calculated broadened LDOS for different species, as described more fully in the text. The experimental spectra form the adsorbed species [5] were recorded at a polar emission angle of 30° in two different polarisation directions (red and blue spectra).

The alignment of the energies of the experimental and theoretical spectra is some somewhat arbitrary due to their different reference energies, and has been chosen in the figure to give the best overall alignment. The overall energy range of the peaks in the theory is smaller than that in the UP spectrum by ~2 eV, whereas the energy range of the states predicted in the old MO calculations is larger than that of the UP spectrum by ~ 1 eV. However, our calculated LDOS clearly reproduces all the main features of the

experimental spectrum with the exception of the splitting of peaks in the UP spectrum at a binding energy ~12 eV relative to the vacuum level. Note, in particular, that the theory shows the same splitting of the most weakly-bound states as that seen in the experimental spectrum.

On the right of Fig. 7 is shown a similar comparison of the experimental UP difference spectra of the adsorbed species on TiO_2(110) formed by exposure to azobenzene with the calculated broadened LDOS for three surface phases, namely adsorbed aniline, adsorbed phenyl imide, and adsorbed C_6H_4NH. The absolute energies of the experimental and theoretical spectra have been aligned to give the best agreement for the two (most core-like) peaks with the largest binding energies. For molecular adsorbate systems, of course, UP spectra contain features due to the substrate as well as due to the molecular orbitals of the adsorbate. It is therefore common practice to regard the difference spectrum – the spectrum obtained in the presence of the adsorbate minus the spectrum obtained from the clean surface – as the best indication of the molecular orbital energies of the adsorbate. Of course, one difficulty in this procedure is that the difference spectrum always contains negative excursions due to attenuation of substrate emission peaks due to the presence of the overlayer, and these can distort the apparent energies of adsorbate emission peaks. In the case of adsorption of azobenzene on rutile TiO_2(110), experimental data recorded in different emission angles and different light polarisation conditions are found to lead to very significant changes in the difference spectra [5] that are, at least in part, due to variations in the subtracted clean surface spectra. Nevertheless, it is possible to discern approximately the same main peak positions in many of these spectra, despite changes in relative intensities. The UP difference spectra shown in Fig. 7 were obtained from the rutile surface at an emission angle of 30° with the polarisation vector in the [001] (red) and $[1\bar{1}0]$(blue) azimuths,[5] the variation in peak heights in the two spectra being representative of the range seen in spectra recorded at other angles.

Comparison of these difference spectra with the calculated LDOS shows there is quite good agreement with the LDOS for adsorbed aniline in the number of peaks and their approximate energies, with the notable exception of the most weakly-bound state which

is displaced relative to the experimental peak position by ~1.5eV. Notice, though, that this leads to an overall narrowing of the spectral range in the LDOS similar to that found in the gas-phase spectrum. The calculated LDOS for adsorbed phenyl imide and adsorbed C_6H_4NH show significantly more structure in the middle of the energy range which agrees much less well with the experimental spectrum. Other notable features that are not consistent with the experimental spectrum are the splitting of the most-strongly bound state for phenyl imide, and of the most weakly-bound state for C_6H_4NH, neither of which are present in the experimental data recorded on rutile TiO_2(110) in any of the many geometries explored.[5]

Based on the results of Fig. 7 we therefore conclude that the UPS experimental data do appear to be most consistent with adsorbed aniline, but particularly in view of the problems associated with extracting reliable adsorbate data from experimental difference spectra, this result must be, at best, only indicative of the correct solution.

A rather different and more indirect influence of the electronic properties of the surface is manifest in the modifications of the photoelectron binding energies of atomic core levels – the so-called core level shifts (CLS) – in XPS. Calculations of the expected CLS values can be performed using DFT methods (using CASTEP and other codes [16,21,22]), and have been used in this study to investigate the changes in C 1s and N 1s photoelectron binding energies for the different surface species. These calculations were performed using the standard (PW91) DFT codes, but a check with DFT-D on calculations for graphite as a reference material (see below) found a difference of only 0.05 eV; the fact that this value is small is particularly notable in view of the fact that the inclusion of dispersion forces is crucial to describe the interplanar forces in graphite. One further potential source of error in these calculations is the possible interaction between the core-ionised potentials if the unit cell used in the calculations is too small. However, a test on the reference compound TiN used for the N 1s CLS values (see below) found a difference in the N 1s CLS of only 0.04 eV between calculations using unit cells containing 8 and 64 atoms, respectively. The effect of using too small a cell was found to be slightly more significant in the adsorption structures for which the calculated results presented here used the same

primitive c(2x2) cell as for the total energy calculations; a test using a larger (2x2) cell for adsorbed aniline led to a difference of 0.10 eV in the mean C 1s CLS, although changes in the differences of the CLS values for the five constituent C atoms were much smaller than this.

Model	C 1s CLS (eV)	Range (eV)	Gaussian σ (eV) in Fig. 8
phenyl imide	-1.33, -2.74, -1.97, -2.65, -1.99, -2.78	1.45	0.48
$C_6H_5NH+ H_a$	-0.34, -1.52, -1.22, -1.49, -1.27, -1.76	1.42	0.67
C_6H_4NH	-0.33, -1.48, -1.25, -1.47, -1.39, -0.06	1.42	0.47
aniline	0, -1.14, -1.00, -1.01, -1.00, -1.12	1.14	0.70

Table 3. C 1s CLS values for C atoms in sequential order around the ring, starting with the C bonded to the N and secondly with a C bonded to H. Thus, for C_6H_4NH the relative binding energy of the C atoms bonded to a bridging O atom on the surface is the final entry in the list. The energies are relative to the C atom bonded to N in aniline which has the largest photoelectron binding energy; also listed are the Gaussian broadening values used in the spectral simulations of Fig. 8.

In the case of the C 1s emission, the inequivalence of the differently-bonded C atoms within the phenyl (or modified-phenyl) ring leads to several different CLS components in the C 1s XP spectrum, which influences the measured spectral line shape. The calculated individual CLS values for the four principal models are given in Table 3. Both the range and the distribution of CLS values differ for these models. For example, the overall range of values is smallest for adsorbed aniline which also has five of the six C atoms (all those not bonded to N) with CLS values in the narrow range of only 0.14 eV. By contrast, in adsorbed phenyl imide these five C atoms have their CLS values in two groups that differ in energy by ~0.7 eV. In order to compare the consequence of these different values with the experimental results, however, one needs some knowledge of the instrumental resolution as well as the intrinsic lifetime broadening and asymmetry of the various components. Unfortunately, this information is not available. Without this we cannot, for

example, test the prediction that the overall peak width should be narrower for adsorbed aniline than for the other species, because the experimental peak width is determined by a convolution of the distribution of CLS values and the (unknown) broadening functions. Nevertheless, some plausible and simplistic assumptions do allow us to establish whether any of the different CLS distributions should lead to spectral lineshapes that are unlikely to be consistent with experiment.

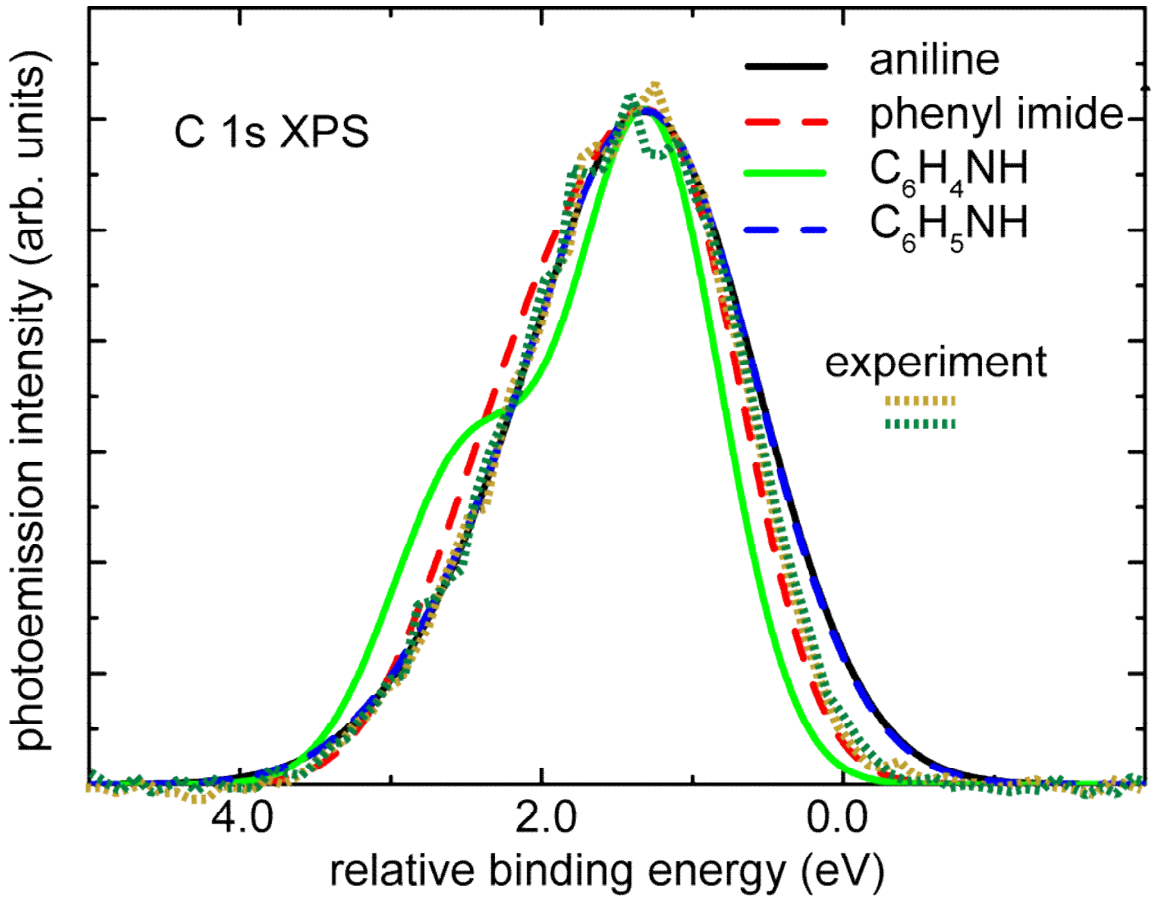

Fig. 8 Comparison of the experimental C 1s XPS lineshape from both aniline and azobenzene reaction with TiO_2(110) [8] with theoretical predictions for the different surface models that assume only Gaussian broadening of the individual CLS components. For each surface species the value of the Gaussian variance was chosen to achieve the same FWHM as the experimental spectra.

In particular, Fig. 8 shows a comparison of the experimental C 1s lineshape (the spectra

obtained from both aniline and azobenzene interaction in the more recent higher-resolution study have been aligned to neglect the very small (~0.1 eV) shift between them [8]), and theoretical simulations based on a sum of Gaussian peaks of equal height at each of the six CLS values in the four different structural models. For each model the Gaussian sigma value (Table 3) has been chosen such as to give a total FWHM (full-width-half-maximum) value for the simulated spectrum equal to that (1.83 eV) of the experimental spectra. Small adjustments of the (arbitrary) energy alignment of the experimental and theoretical spectra have some influence on which simulated spectrum gives the best fit to the experiment, and the exact steepness of the low and high energy sides of the spectrum would be influenced by inclusion of the asymmetry of the true spectral lineshape. However, what is rather clear from Fig. 8 is that the simulated spectrum for adsorbed C_6H_4NH, the energetically-favoured solution from reaction of pure azobenzene with a clean TiO_2 surface, is quite different from the experimental lineshape. In particular, this species leads to a spectrum with a very distinct shoulder that is not seen in the experiment. It therefore appears that this structural solution is not consistent with the XPS lineshape data.

Model	C 1s CLS (eV)	C 1s mean (eV)	N 1s (eV)
phenyl imide	-0.20, -1.51, -0.74, -1.42, -0.76, -1.55	283.6	395.5
$C_6H_5NH+ H_a$	0.89, -0.29, 0.01, -0.26, -0.04, -0.53	284.6	397.5
C_6H_4NH	0.90, -0.25, -0.02, -0.24, -0.16, 0.11	284.7	397.7
aniline	1.23, 0.09, 0.23, 0.22, 0.23, 0.11	285.0	400.2
experiment		285.3	400.5

Table 4 Calculated C 1s individual CLS relative to graphite, and absolute (mean) C 1s and N 1s photoelectron binding energies, based on experimental values for graphite and TiN, respectively, of 284.6 eV and 397.2 eV. Also shown are the experimental values for the surface species formed by azobenzene and aniline reaction with TiO_2(110).[4]

One further important piece of information in XPS data is the *absolute* photoelectron binding energies of the C 1s and N 1s emission. Unfortunately, pseudopotential DFT

calculations do not provide these absolute values, but with the introduction of a reliable experimental reference value, the calculated CLS values relative to this reference system can then be used to give absolute binding photoelectron energies for the adsorbate structures studied here. For this purpose we have taken the photoelectron binding energies of C 1s in graphite (284.6 eV) and of N 1s in TiN (398.2 eV); in each case reported values from several measurements [23] have a small scatter, but these values are unlikely to be in error by more than 0.2 eV . Table 4 shows the absolute C 1s and N 1s photoelectron binding energies calculated in this way, compared with the experimental values.[4] For C 1s the spread of predicted energies for three of the different surface models is only 0.4 eV, so bearing in mind possible errors in the combination of the reference calibration and the calculated CLS values of a few tenths of an eV, this variation may not be an entirely reliable basis for identifying a single model. Nevertheless, it is notable that the best agreement (with a discrepancy of only 0.3 eV) with experiment is for adsorbed aniline, whereas for phenyl imide the discrepancy is 1.7 eV. For the N 1s photoelectron binding energy the results are far more significant, because the range of calculated energies for the 4 models is 5.0 eV. In this case, too, the prediction for the measured energy for adsorbed aniline differs from the experimental value by 0.3 eV, but the next nearest calculated value, for C_6H_4NH, differs from the experimental value by 2.8 eV, while for phenyl imide the difference is 5.0 eV. The combination of these two adsorbate absolute binding energies thus provides very strong support for the surface species present in the experiments being adsorbed aniline.

4. Discussion and conclusions

The experimental evidence for there being a common surface species formed by the interaction of TiO_2(110) with either azobenzene or aniline is strong. In both cases the ordering, as seen in LEED and STM is the same,[4] the XP [4,8] and UP [5] spectra are the same, and the NEXAFS and N 1s PhD data [8] are the same. On this basis it was proposed that the common species is phenyl imide, C_6H_5N-, produced by scission of the N=N bond in azobenzene, or by dehydrogenation of the N atom in aniline.[4] Unfortunately, both earlier [9,10] calculations, and the new results presented here, show that this is not

energetically favoured for azobenzene; the exact size of the amount of extra energy needed to effect this dissociation depends on the influence of dispersion forces, but a value ~3 eV is so large that the conclusion that this reaction should not occur seems irrefutable. Our calculations show that the energy increase required for the dehydrogenation of aniline to form a phenyl imide surface intermediate is even larger. For azobenzene our results indicate that N=N bond scission, combined with rearrangement of the H atoms in the fragment to produce adsorbed C_6H_4NH, *is* energetically favourable (though we have not investigated the possible energy barrier to this rearrangement). However, a large increase in energy is required for the formation of this surface species from gas-phase aniline. It is therefore clear that neither phenyl imide nor adsorbed C_6H_4NH can be the *common* surface intermediate. What our DFT calculations show, however, is that adsorbed intact aniline is much the most energetically favoured surface species after interaction with aniline in the gas phase, and that this same surface species is energetically preferred over adsorbed C_6H_4NH following interaction with azobenzene, *if there is a source of sufficient hydrogen*. Notice that the relative energies presented in Table 2 also show that each successive addition of each of the two H atoms required leads to a lowering of the energy; adsorbed $C_6H_5NH_2$ has lower energy than adsorbed C_6H_5NH + H_a, which has lower energy than adsorbed C_6H_4NH with hydrogen either in the gas phase or on the surface.

The evidence that aniline is the common surface species formed in the experiments using the two different reactants is strong. The calculated adsorption site, Ti-N bondlength and molecular orientation are consistent with the experimental PhD and NEXAFS data. A comparison of calculated LDOS with the experimental UP spectra marginally favours this species, and the absolute XPS C 1s and N 1s binding energies provide strong support for the presence of this species.

The key issue is thus this: in the case of azobenzene reaction with TiO_2(110), what is the source of the 1 ML of H atoms needed to react with 0.25 ML azobenzene and create 0.5 ML of surface aniline to form a c(2x2) overlayer? In fact a nominally clean TiO_2(110) surface in UHV almost always does have some adsorbed H atoms present, because a low

concentration of bridging oxygen vacancies reacts with residual water in the gas phase, each vacancy leading to two bridging OH species. However, even if the surface vacancy concentration is 10% (the upper end of the range expected for a well-prepared surface) the resulting H coverage is only 0.2 ML, much less than the 1 ML required. Li and Diebold also remarked [4] that the bulk oxide must be considered as a reservoir for H atoms at the surface due to evidence that H atoms can readily move to the subsurface.[19] It is difficult to estimate the amount of hydrogen that could be supplied to the surface in this way. It is also possible, however, that the gas phase may be a source of hydrogen, even under the nominal UHV conditions of the experiments. In particular, dosing of the surface with molecules from the gas phase is normally performed with the operation of at least an ion gauge, and often also a mass spectrometer, in order to monitor the exposure. In both cases the ionising filaments lead to fragmentation of the gas-phase species, so cracking of gas-phase azobenzene must lead to a significant partial pressure of hydrogen, including atomic and excited species.

In this context it is interesting to note that the NEXAFS study of a multilayer of azobenzene at low temperature found that on heating the film to above room temperature, to produce a single molecular layer, the spectra recorded indicated that at least some of this molecular layer was of intact azobenzene. Forming the single molecular layer in this way, with a higher sticking factor due to the low temperature, would lead to less exposure of the bare titania surface to gas-phase molecular fragments, and could account for this difference. The other circumstances under which intact azobenzene was reported to be present on TiO_2(110) at room temperature was in STM imaging at very low coverage (~0.02 ML). In this case one might argue that there should be ample surface hydrogen, arising from water interaction with surface vacancies, for reaction of the azobenzene to aniline, if the surface mobility was sufficient. On the other hand, the sticking factor of the azobenzene at very low coverage may be expected to be much higher than at near-saturation coverage, so if a flow of hydrogen from gas-phase fragmentation is required, the exposure time may prove to be inadequate. Moreover, the observation in the recent experimental study that it proved more difficult to achieve a high coverage of the molecular reaction product using exposure to azobenzene than to aniline could be

attributed to an insufficient supply of hydrogen.

In conclusion, the results of our DFT calculations show that the formation of phenyl imide on TiO_2(110) from N=N bond scission of azobenzene, or from dehydrogenation of aniline, is strongly energetically disfavoured. However, the formation of adsorbed aniline from exposure to gas-phase aniline, or by reaction with azobenzene in the presence of a source of hydrogen, is strongly energetically favoured. Moreover, only the structural and electronic properties of a c(2x2) phase adsorbed aniline on this surface are consistent with all available experimental data. However, the origin of the source of hydrogen required for azobenzene reaction in these experiments remains unclear. Further experiments to explore this issue appear to be warranted. For example, there is some evidence that an adsorbed intact azobenzene layer may be obtained by initial multilayer deposition at low temperature, followed by thermal desorption of the excess. If this proves to be correct, further experiments introducing hydrogen in different ways could provide further insight into the mechanism of hydrogenation of azobenzene. However, whatever is the outcome of such experiments, our results strongly indicate that adsorbed intact aniline is a key surface intermediate in the hydrogenation of azobenzene, and the reduction of aniline, over TiO_2(110).

Acknowledgements

The authors acknowledge the partial support of the Engineering and Physical Sciences Research Council (UK) for this work in the form of studentship funding. The computing facilities were provided by the Centre for Scientific Computing of the University of Warwick with support from the Science Research Investment Fund. Shao-Chun Li is thanked for providing a copy of the original UPS figure from ref [5].

References

1 Haruta, M. Size- and Support Dependency in the Catalysis of Gold, *Catal. Today* 1997,*36*, 153-166.

2 Corma, A.; Serna, P. Chemoselective Hydrogenation of Nitro Compounds with Supported Gold Catalysts, *Science* **2006**, *313*, 332-334.

3 Grirrane, A.; Corma, A.; Garcia, H. Gold-Catalyzed Synthesis of Aromatic Azo Compounds from Anilines and Nitroaromatics, *Science*, **2008**, *322*, 1661-1664.

4 Li, S.-C.; Diebold, U. Reactivity of TiO_2 Rutile and Anatase Surfaces Toward Nitroaromatics, *J. Am. Chem. Soc*., **2010**, *132*, 64-66.

5 Li, S.-C.; Losovyj, Y.; Paliwal, V.K.; Diebold, U. Photoemission Study of Azobenzene and Aniline Adsorbed on TiO_2 Anatase (101) and Rutile (110) Surfaces, *J. Phys. Chem. C*, **2011**, *115*, 10173-10179.

6 Woodruff, D.P.; Bradshaw, A.M. Adsorbate Structure Determination on Surfaces Using Photoelectron Diffraction, *Rep. Prog. Phys.*,**1994**, *57*, 1029-1080.

7 Woodruff, D.P. Adsorbate Structure Determination Using Photoelectron Diffraction, *Surf. Sci. Rep*., **2007**, *62*, 1-38.

8 Kreikemeyer-Lorenzo, D.; Unterberger, W.; Duncan, D.A.; Lerotholi, T.J.; Woodruff, D.P. The Local Structure of the Azobenzene/Aniline Reaction Intermediate on TiO_2-(110), *Surf. Sci*., **2013**, *613*, 40-47.

9 Prates Ramalho, J.P.; Illas, F. Theoretical Study of the Adsorption and Dissociation of Azobenzene on the Rutile TiO_2(1 1 0) Surface,*Chem. Phys. Lett*., **2011**, *501*, 379-384.

10 Prates Ramalho, J.P.; Illas, F. Assessing the Importance of Van Der Waals Interactions on the Adsorption of Azobenzene on the Rutile TiO_2(110) Surface, *Chem. Phys. Lett.*, **2012**, *545*, 60-65.

11 Prates Ramalho, J.P.;. Illas, F. Erratum to ‘‘Assessing the Importance of Van Der Waals Interactions on the Adsorption of Azobenzene on the Rutile TiO_2(110) Surface’’ [Chem. Phys. Lett. 545 (2012) 60], *Chem. Phys. Lett.*, **2013**, *557*, 194..

12 Clark, S.J.; Segall, M.D.; Pickard, C.J.; Hasnip, P.J.; Probert, M.J.; Refson, K.; Payne, M.C. First Principles Methods Using CASTEP, *Z Kristallogr*., **2005**, *220*, 567-570.

13 Perdew, J.P.; Burke, K.; Wang, Y. Generalized Gradient Approximation for the Exchange-Correlation Hole of a Many-Electron System, *Phys. Rev. B*, **1996**, *54*, 16533-16539.

14 Ortmann, F.; Bechstedt, F.; Schmidt, W.G. Semiempirical Van Der Waals Correction to the Density Functional Description of Solids and Molecular Structures. *Phys. Rev. B*, **2006**, *73*, 205101-1-10.

15 McNellis, E.R.; Meyer, J.; Reuter, K.; Azobenzene at Coinage Metal Surfaces: Role of Dispersive Van Der Waals Interactions. *Phys. Rev. B* , **2009**, *80*, 205414-1-10.

16 Gao, S.-P.; Pickard, C.J.; Perlov, A.; Milman, V. Core-Level Spectroscopy Calculation and the Plane Wave Pseudopotential Method. *J. Phys.: Condens. Matter*, **2009**, *21*, 104203-1-12.

17 Kowalski, P.M.; Meyer, B.; Marx, D. Composition, Structure, and Stability of the Rutile Tio_2(110) Surface: Oxygen Depletion, Hydroxylation, Hydrogen Migration, and Water Adsorption. *Phys. Rev. B*, **2009**, *79*, 115410-1-16.

18 Abrahams, S.C.; Bernstein, J.L. Rutile: Normal Probability Plot Analysis and Accurate Measurement of Crystal Structure . *J. Chem. Phys.*, **1971**, *55*, 3206-3212.

19 Yin, X.-L.; Calatayud, M.; Qiu, H.; Wang, Y.; Birkner, A.; Minot, C.; Wöll, Ch. Diffusion Versus Desorption: Complex Behavior of H Atoms on an Oxide Surface. *ChemPhysChem*, **2008**, *9*, 253-256.

20 Palmer, M.H.; Moyes, W.; Spiers, M.; Rudyard, J.N.A. The Electronic Structure of Substituted Benzenes; A Study of Aniline, the Toluidines, Phenylenediamines and Fluoroanilines by Photoelectron Spectroscopy and Ab Initio Calculations. *J. Mol. Struct.*, **1979**, *53*, 235-249.

21 Pehlke, E.; Scheffler, M. Evidence for Site-Sensitive Screening of Core Holes at the Si and Ge (001) Surface. *Phys. Rev. Lett.*, **1993**, *71*, 2338-2341.

22 Pasquarello, A.; Hybertsen, M.S.; Car, R. Si 2p Core-Level Shifts in Small Molecules: A First Principles Study. *Phys. Scr.*, **1996**, *T66*, 118-120.

23 Naumkin, A.V.; Kraut-Vass, A.; Gaarenstroom, S.W.; Powell C.J. *NIST X-ray Photoelectron Spectroscopy Database, NIST Standard Reference Database 20, Version 4.1*, NIST, Gaithersburg, MD, USA, 2012.